

AD-A240 627

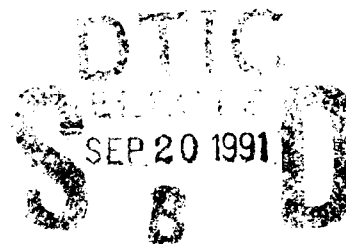


WL-TR-91-4050



**A COMPARISON OF SINGLE CYCLE OVERLOAD EFFECT ON
Al-Li 2091-T81 PLATE AND 2091-T83 SHEET**

Russell R. Cervay and Kumar V. Jata
University of Dayton Research Institute
300 College Park Avenue
Dayton, OH 45469-0136



AUGUST 1991

Interim Report for the Period November 1990 - January 1991

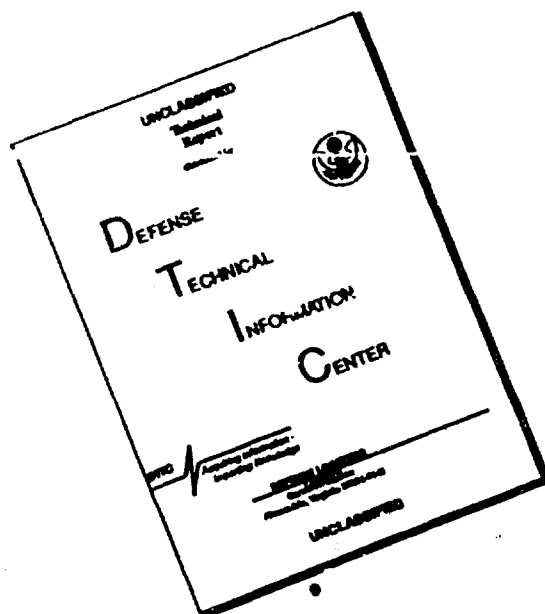
Approved for Public Release; Distribution Unlimited.

MATERIALS DIRECTORATE
WRIGHT LABORATORY
AIR FORCE SYSTEMS COMMAND
WRIGHT-PATTERSON AIR FORCE BASE, OH 45433-6533

91-10847



DISCLAIMER NOTICE



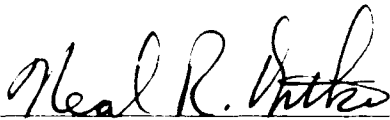
**THIS DOCUMENT IS BEST
QUALITY AVAILABLE. THE COPY
FURNISHED TO DTIC CONTAINED
A SIGNIFICANT NUMBER OF
PAGES WHICH DO NOT
REPRODUCE LEGIBLY.**

NOTICE

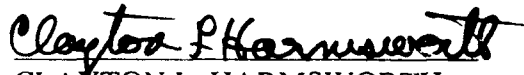
When Government drawings, specifications, or other data are used for any purpose other than in connection with a definitely Government-related procurement, the United States Government incurs no responsibility or any obligation whatsoever. The fact that the Government may have formulated or in any way supplied the said drawings, specifications, or other data, is not to be regarded by implication, or otherwise in any manner construed, as licensing the holder, or any other person or corporation; or as conveying any rights or permission to manufacture, use, or sell any patented invention that may in any way be related thereto.

This report is releasable to the National Technical Information Service (NTIS). At NTIS, it will be available to the general public, including foreign nations.

This technical report has been reviewed and is approved for publication.

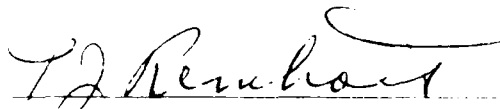


NEAL R. ONTKO
Contractor Monitor
Engineering and Design Data
Materials Engineering Branch

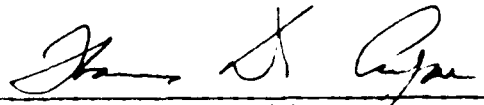


CLAYTON L. HARMSWORTH
Technical Manager
Engineering and Design Data
Materials Engineering Branch

FOR THE COMMANDER



T.J. REINHART, Chief
Materials Engineering Branch
Materials Directorate



THOMAS D COOPER, Chief
Systems Support Division
Materials Directorate

If your address has changed, if you wish to be removed from our mailing list, or if the addressee is no longer employed by your organization, please notify WL/MLSE, Wright-Patterson AFB, OH 45433-6533 to help us maintain a current mailing list.

Copies of this report should not be returned unless return is required by security considerations, contractual obligations, or notice on a specific document.

UNCLASSIFIED

SECURITY CLASSIFICATION OF THIS PAGE

Form Approved
OMB No 0704 0188

REPORT DOCUMENTATION PAGE

1a REPORT SECURITY CLASSIFICATION UNCLASSIFIED		1b RESTRICTIVE MARKINGS	
2a SECURITY CLASSIFICATION AUTHORITY		3 DISTRIBUTION/AVAILABILITY OF REPORT Approved for Public Release; distribution Unlimited.	
2b DECLASSIFICATION/DOWNGRADING SCHEDULE			
4 PERFORMING ORGANIZATION REPORT NUMBER(S) UDR-TR-91- 16		5. MONITORING ORGANIZATION REPORT NUMBER(S) WL-TR-91- 4050	
6a NAME OF PERFORMING ORGANIZATION University of Dayton Research Institute	6b OFFICE SYMBOL (If applicable)	7a NAME OF MONITORING ORGANIZATION Materials Directorate (WL/MLSE) Wright Laboratory	
6c ADDRESS (City, State, and ZIP Code) 300 College Park Dayton, Ohio 45469-0138		7b ADDRESS (City, State, and ZIP Code) Wright- Patterson AFB, Ohio 45433-6533	
8a NAME OF FUNDING/SPONSORING ORGANIZATION	8b OFFICE SYMBOL (If applicable)	9 PROCUREMENT INSTRUMENT IDENTIFICATION NUMBER F33615-90-C-5915	
8c ADDRESS (City, State, and ZIP Code)		10 SOURCE OF FUNDING NUMBERS	
		PROGRAM ELEMENT NO 62102F	PROJECT NO 2418
		TASK NO 04	WORK UNIT ACCESSION NO 81
11 TITLE (Include Security Classification) A Comparison of Single Cycle Overload Effect on Al-Li 2091-T81 Plate and 2091-T83 Sheet			
12 PERSONAL AUTHOR(S) Russell R. Cervay and Dr. Kumar V. Jata			
13a TYPE OF REPORT Interim	13b TIME COVERED FROM 11-90 TO 1-91	14. DATE OF REPORT (Year, Month, Day) August 1991	15 PAGE COUNT 31
16 SUPPLEMENTARY NOTATION			
17 COSATI CODES		18 SUBJECT TERMS (Continue on reverse if necessary and identify by block number)	
FIELD	GROUP	Overload Fatigue Crack Growth	
		Retardation Crack Closure	
		Al Alloy 2091	
19 ABSTRACT (Continue on reverse if necessary and identify by block number) Previous researchers have established that for identical fatigue test conditions fatigue crack growth rate in aluminum-lithium alloy 2091 plate is far slower than in sheet, due to the development of a coarser fracture surface in the plate producing crack tip shielding resulting in a reduced effective crack driving parameter. Based on these results one would anticipate the plate material to exhibit a greater number of post-overload delay cycles than the sheet. This study was undertaken to quantify the effect of a single tensile overload fatigue cycle on the crack velocity of both product forms. The test procedure consisted of shedding the dynamic loads to a stress intensity range of 6 KSI/in where a single 60 percent overload fatigue cycle was applied, followed by resumption of the pre-overload loading conditions. Following the overload, cyclic loads were periodically adjusted to maintain a constant stress intensity range of 6 KSI/in. Other test conditions, including specimen thickness and yield (Continued on other side)			
20 DISTRIBUTION/AVAILABILITY OF ABSTRACT <input checked="" type="checkbox"/> UNCLASSIFIED/UNLIMITED <input type="checkbox"/> SAME AS RPT <input type="checkbox"/> DTIC USERS		21 ABSTRACT SECURITY CLASSIFICATION UNCLASSIFIED	
22a NAME OF RESPONSIBLE INDIVIDUAL Neal R. Ontko		22b TELEPHONE (Include Area Code) (513) 255-5128	22c OFFICE SYMBOL WL/MLSE

19. ABSTRACT (Continued)

strength were nearly identical. The plate material showed more retardation than the sheet, as it required far more post-overload fatigue cycles to recover the pre-overload velocity. The number of delay cycles decreased when the crack length prior to the application of overload was longer. The pre-overload crack closure load was higher in the plate and the velocity was an order of magnitude lower. Following the overload, there was little to no change in the crack closure load in either material and that remained true throughout the recovery period.

TABLE OF CONTENTS

<u>SECTION</u>		<u>PAGE</u>
1	INTRODUCTION	1
2	MICROSTRUCTURE AND TENSILE PROPERTIES	3
3	FATIGUE CRACK PROPAGATION BEHAVIOR OF THE 2091 PLATE VS. SHEET	6
4	OVERLOAD TEST PROCEDURE	8
5	RESULTS AND DISCUSSION	9
6	CONCLUDING REMARKS	21
7	REFERENCES	22



Accession For	
NTIS GRA&I	<input checked="" type="checkbox"/>
DTIC TAB	<input type="checkbox"/>
Unannounced	<input type="checkbox"/>
Justification	
By	
Distribution/	
Availability Codes	
Dist	Avail and/or Special
A-1	

LIST OF FIGURES

<u>FIGURE</u>		<u>PAGE</u>
1	Micrographs of the Grain Structure in the 0.144 Inch Sheet of 2091-T83 at 100X	4
2	Micrographs of the Grain Structure in Half-Inch Thick 2091-T81 Plate at 100X	4
3	A Comparison of FCG Rates in L-T and T-L Orientations for 2091 Sheet. Naturally Aged (T3) and Artificially Aged, to 500 Hours at 135°C are Also Shown.	7
4	A Comparison of Delay Cycles Due to Fatigue Crack Growth Retardation for a 60 Percent Overload Cycle at a Stress Intensity of 6 KSI√in in 2091-T81 Plate Versus 2091-T83 Sheet. Thickness of the Compact Tension Specimens Used for Plate and Sheet was 0.144 Inch.	11
5	Delay Cycles Due to Fatigue Crack Growth Retardation for an 80 Percent Overload Cycle at a Stress Intensity Range of 6 KSI√in, in 2091-T81 Plate, with a Specimen Thickness of 0.250 Inch.	12
6	A Comparison of the Crack Closure Level Prior to the Application of 60 Percent Overload Cycle. Note the Larger Level of Crack Closure in the Plate as Compared to the Sheet Which Correlates With the Overload Delay Cycles in Figure 2.	13
7	(a) Fatigue Crack in Alloy 2091-T81 Plate, and (b) in Alloy 2091-T83 Sheet at 100X	14
8	(a) Fatigue Crack Growth Rates and (b) Normalized Crack Closure Levels in 2091-T8 Sheet and Plate, in the L-T Orientation at R=0.1, as a Function of Stress Intensity Range. Reproduced from Reference (1).	15
9	Crack Velocity Versus Post-Overload Crack Extension for Alloy 2091-T83 Sheet	18

LIST OF FIGURES (Concluded)

<u>FIGURE</u>		<u>PAGE</u>
10	Crack Velocity Versus Post-Overload Crack Extension for Alloy 2091-T81 Plate 0.144 Inch Thick	19
11	Crack Velocity Versus Post-Overload Crack Extension for Alloy 2091-T81 Plate 0.250 Inch Thick	20

LIST OF TABLES

<u>TABLE</u>		<u>PAGE</u>
1	Chemical Composition of 2091 Al-Li Alloy in Weight Percent	3
2	Comparison Between 2091 Plate and 2091 Sheet	3
3	Tensile Properties of 2091 Sheet and Plate	5
4	Post-Overload Fatigue Test Results for 2091 Plate and Sheet	10
5	Post-Overload Recovery Crack Extension in 2091 Plate and Sheet	17

PREFACE

This technical report represents work conducted by the University of Dayton Research Institute under contract to the Wright Research and Development Center, Materials Laboratory, Systems Support Division, Contract F33615-90-C-5915, "Quick Reaction Evaluation of Materials." Mr. Neal Ontko was the contract monitor.

This effort was conducted during the period of November 1990 to January 1991. The authors, Russell Cervay and Dr. Kumar V. Jata, would like to extend recognition to Messrs. John Eblin and Robert Hicks of the University of Dayton who exercised care in instrumenting the test specimens and in conducting the tests.

This report was submitted by the authors for publication in April 1991.

SECTION 1 INTRODUCTION

It is already well known that ingot-metallurgy aluminum lithium alloys exhibit substantially superior fatigue crack growth resistance in comparison to the conventional 7xxx and 2xxx alloys. A number of factors have been attributed to this markedly slower growth rate in aluminum lithium alloys. Higher elastic modulus, more reversible slip and larger degree of out-of-plane fatigue cracking are among the chief factors that have been proposed for the superior fatigue crack growth resistance of aluminum lithium alloys in comparison to traditional aluminum alloys. As is well known higher elastic modulus (and lower density) in aluminum lithium alloys is derived from lithium additions to the alloy. Aluminum lithium plate alloys are usually unrecrystallized due to zirconium additions and exhibit large grain size with a high degree of planar slip. Planar slip in these alloys aids cracks to propagate in out-of-plane. The increased distances to which out-of-plane cracking occurs are due to large grain size. Since planar slip can aid reversibility of slip ahead of the crack tip, it has been attributed to slower crack growth rates in aluminum lithium alloys. On the other hand, the large degree of out-of-plane cracking causes a substantial amount of roughness-induced crack closure in these alloys. Thus the crack closure levels in plate alloys have been reported to be extremely high, approximately 80 percent of the nominal crack driving force in the near-threshold region, which tremendously reduces fatigue crack growth rates.

Recently a study (1) comparing the fatigue crack growth rates between 2091 aluminum lithium plate and sheet alloys was conducted to demonstrate the differences between the two product forms. Microstructurally the two product forms differ. Aluminum lithium sheet alloys are prone to recrystallization during processing and thus exhibit a recrystallized microstructure. The recrystallized microstructure of the sheet is far more isotropic than the plate alloy and thus exhibits far less planar slip. Thus out-of-plane fatigue crack growth is far less in sheet, resulting in reduced roughness-induced crack closure and higher fatigue crack growth rates than the corresponding plate alloy.

Crack-tip-shielding effect which takes the form of roughness-induced crack closure in aluminum lithium alloys has also been shown to play a key role in determining the number of delay cycles. The number of delay cycles are the number of cycles for the crack to attain the same pre-overload fatigue crack growth rate after an overload is applied.

However, studies showing how a single overload (OL) fatigue cycle would affect the subsequent crack growth rates in aluminum-lithium plate versus sheet are lacking. The present study was aimed to quantify the effects of a single overload fatigue cycle on the crack growth rates in a 2091 plate and sheet of comparable strength.

SECTION 2
MICROSTRUCTURE AND TENSILE PROPERTIES

Commercially produced 2091 Al-Li alloys used in this study were obtained from ALCOA. The alloy in the plate form was obtained in a T81 temper, whereas, the sheet was in a naturally aged, T3, temper. The as-received thickness of the plate was 0.5 inch (12.7 mm) and that of the sheet was 0.144 inch (3.2 mm). The nominal chemical composition of product forms is shown in Table 1.

TABLE 1
CHEMICAL COMPOSITION OF 2091 Al-Li ALLOY
IN WEIGHT PERCENT

<u>Li</u>	<u>Cu</u>	<u>Mg</u>	<u>Zr</u>	<u>Fe</u>	<u>Si</u>	<u>Mn</u>	<u>Ti</u>	<u>Al</u>
2.0	2.1	1.5	0.1	0.3	0.2	0.1	0.1	Bal.

Differences in the grain structure between the two product forms are clearly borne out in the optical micrographs, Figures 1 and 2. Apart from these differences between the plate and sheet several other dissimilarities also exist between plate and sheet for aluminum lithium alloys. These are listed below in Table 2.

TABLE 2
COMPARISON BETWEEN 2091 PLATE AND 2091 SHEET

<u>2091 Plate</u>	<u>2091 Sheet</u>
1. large grain size; unrecrystallized	1. smaller grain size; partially recrystallized
2. strong texture	2. random texture
3. more fracture surface roughness induced crack closure	3. less fracture surface roughness induced crack closure
4. anisotropic microstructure	4. isotropic microstructure

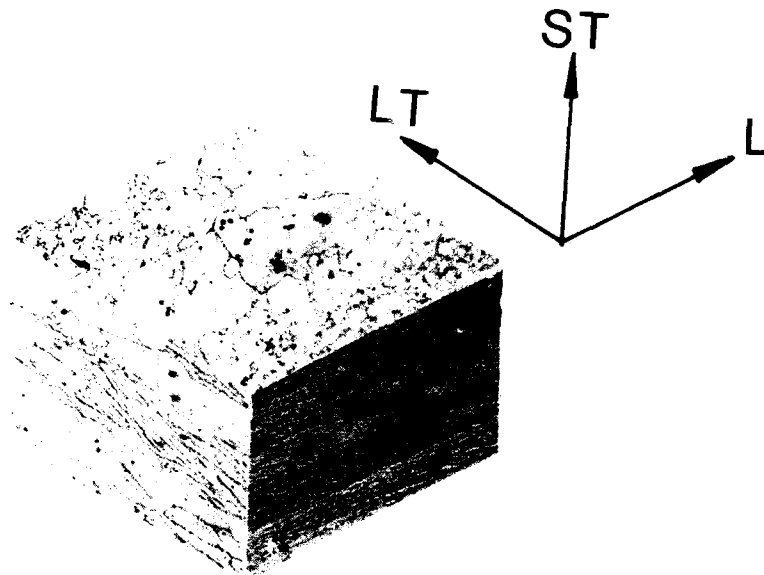


Figure 1. Micrographs of the Grain Structure in the 0.144 Inch Sheet of 2091-T83 at 100X.

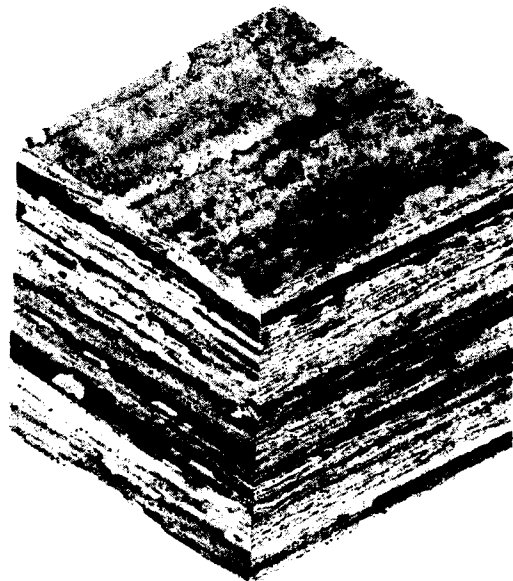


Figure 2. Micrographs of the Grain Structure in Half-Inch Thick 2091-T81 Plate at 100X.

Since the goal of this study was to understand the mechanisms behind the effect of a single overload cycle on the fatigue crack growth retardation, variables such as yield strength and specimen thickness of the two product forms were kept constant.

As the sheet was obtained in a naturally aged, T3, condition an additional heat treatment was given so as to make the yield strength of the sheet equivalent to that of the plate. An aging temperature of 135°C (275°F) was chosen and the material was aged for various numbers of hours up to 500 hours to promote additional precipitation hardening. Tensile properties of the sheet and plate are shown in Table 3. For the compact tensions used in overload experiments, an aging treatment of 500 hours at 135°C was used.

TABLE 3
TENSILE PROPERTIES OF 2091 SHEET AND PLATE

<u>Temper</u>	<u>Yield Strength (MPa)</u>	<u>UTS (MPa)</u>	<u>Elongation (%)</u>
		<u>2091 Sheet</u>	
T3	348	419	19.2
12 hrs @ 135°C	369	437	15.7
500 hrs @ 135°C	415	449	12.9
		<u>2091 Plate</u>	
T8	436	521	9

SECTION 3
FATIGUE CRACK PROPAGATION BEHAVIOR
OF THE 2091 PLATE VS. SHEET

It is now well established that the fatigue crack growth resistance in Al-Li plate product form is much higher than in thin sheet product.⁽¹⁾ For a given yield strength and specimen thickness, crack growth rates in plate have been shown to be lower by an order of magnitude at a given stress intensity range. The lower crack growth velocities in the plate have been attributed to the larger crack closure levels that develop in the plate material. For 2091 alloy it has been reported⁽¹⁾ that crack closure values in plate are 80 percent as compared to 50 percent in sheet at a stress intensity range of 6 KSI $\sqrt{\text{in}}$. In this laboratory, for the same thickness of 2091 plate and sheet, far-field crack closure values established using a back-face strain gage of 65 percent and 51 percent have been obtained at 6 KSI $\sqrt{\text{in}}$.

In a previous effort⁽²⁾ fatigue crack growth data was obtained on the naturally aged and heat treated tempers which included the same aging at 135°C for 12 hours and 500 hours. Fatigue crack growth rates, Figure 3, did not differ much for the various tempers⁽²⁾ in spite of an increase in tensile strength.

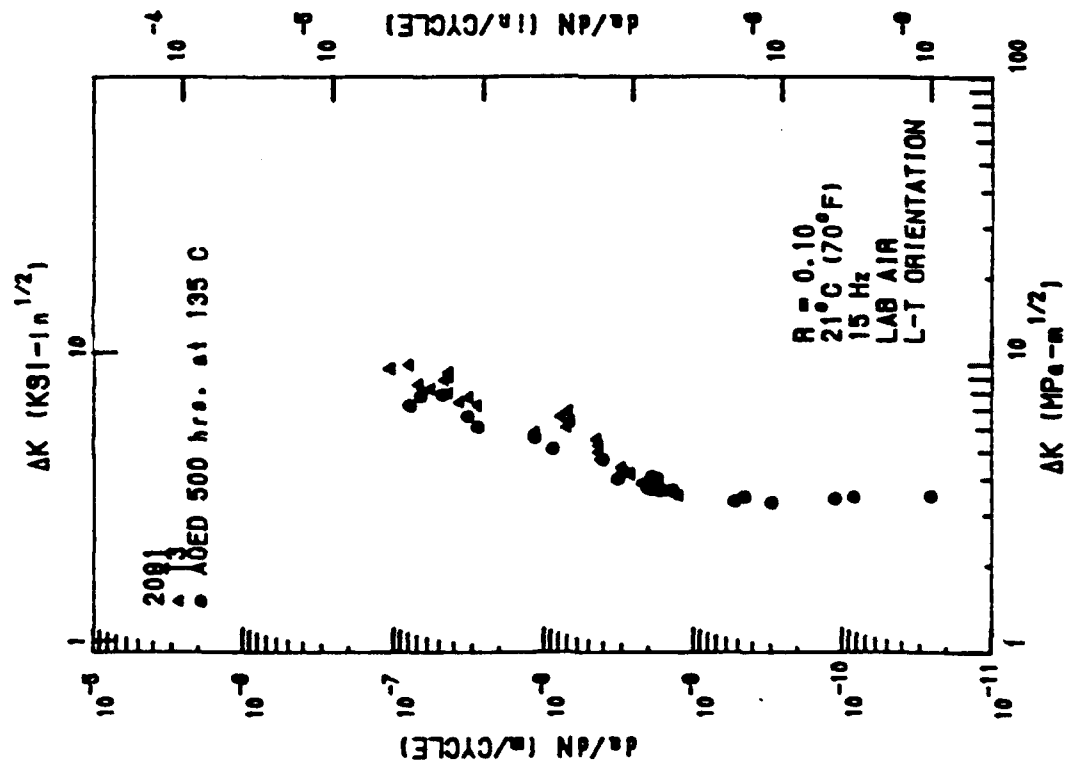
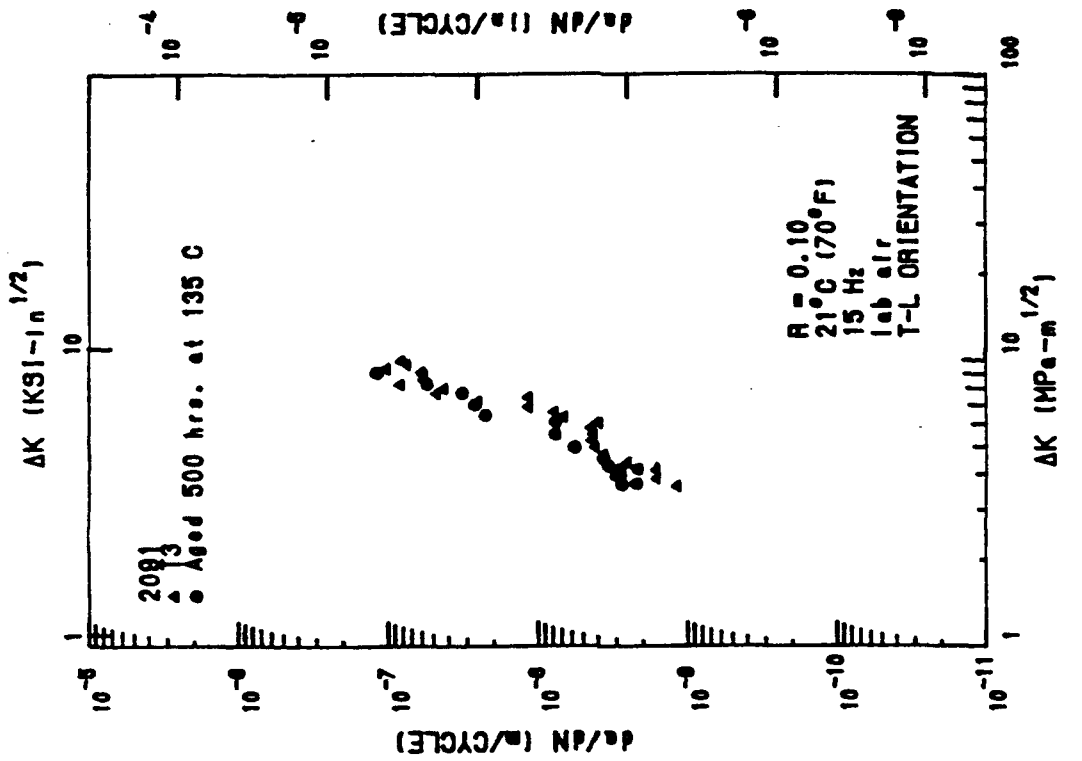


Figure 3. A Comparison of FCG Rates in L-T and T-L Orientations for 2091 Sheet. Naturally Aged (T3) and Artificially Aged, to 500 Hours at 135°C, are also shown.

SECTION 4 OVERLOAD TEST PROCEDURE

Compact tension specimens with a width equal to 1.5 inch were tested in the L-T orientation. In order to eliminate the effect of specimen thickness on fatigue crack growth, the same thickness of 3.2 mm was maintained for both plate and sheet. All tests were conducted at a load ratio of 0.05 at a frequency of 15 Hz. Crack length was measured using Fractomat Krak Gage. Crack opening load was measured using the dual back-face strain gage technique as previously discussed.⁽³⁾ The test procedure consisted of shedding the cyclic load by 10 percent for every 0.01-inch crack extension. When the stress intensity range was within 7 percent of the target value ($6 \text{ KSI}\sqrt{\text{in}}$), a 5 percent drop in the load was adjusted and a crack extension of 10 mils was allowed at this stress intensity range. This was followed by a single 60 percent fatigue overload cycle and then pre-overload cyclic loading was resumed. The crack was allowed to attain its pre-overload velocity under a constant stress intensity range condition; i.e., $6 \text{ KSI}\sqrt{\text{in}}$.

SECTION 5 RESULTS AND DISCUSSION

The postoverload delay cycles required for recovery of the preoverload crack velocity versus the normalized crack length, (i.e., a/w) are presented in Table 4 and in Figure 4. Two 80 percent overload tests were performed on the plate material and both resulted in crack arrest. This is the same level of overload used in a previous study⁽⁴⁾ which included limited testing of the 2091 alloy in plate form. In that study, four specimens with a thickness of 0.250 inch were subjected to an 80 percent overload; the cracks always recovered a velocity equal to or exceeding that existing prior to overload as illustrated in Figure 5. That study⁽⁴⁾ employed a specimen thickness of 0.250 inch, whereas in this effort, a thickness of 0.144 inch is used. This may be attributable to the more severe plane stress condition existing in the thinner specimen which generates a larger plastic zone and eventual crack arrest. In the current project one of the 60 percent overload tests on the plate material also arrested; a second required 891,000 post-overload cycles to recover. A 60 percent overload was thus adopted for all remaining tests. The number of postoverload delay cycles diminishes with additional crack length for both materials as shown in Table 4 and Figure 4. The plate product form showed much more retardation than the sheet, as reflected by the increased post-overload delay cycles. "Crack tip shielding"⁽¹⁾, as evident by the higher crack closure levels in the plate as compared to the sheet, is the major mechanism responsible for greater effect in the plate. The crack closure levels are shown in Figure 6 for both plate and sheet. More fracture surface roughness in the plate produces a higher closure load which reduces the local effective stress intensity range at the crack tip. Figure 7(a) contrasts the plate test material fatigue crack branching and out-of-plane deflection to that of the sheet. Figure 7(b). This is evident in Table 4, where, for a constant stress intensity range equal to $6 \text{ KSI}\sqrt{\text{in}}$, preoverload velocities in the sheet are more than an order of magnitude greater than those in the plate for a given crack length. This is similar to the findings in Reference 1 where constant amplitude loading fatigue crack growth data for alloy 2091 in both product forms are presented. Figure 8 is reproduced from that reference. There the closure stress intensity was higher in the plate and showed less scatter. In the current effort, following the overload there was little or no change in the crack closure loads, consistent with the findings of Rao, et al.⁽¹⁾ The largest rise was less than 5 percent and for several of the tests there was no detectable change at all.

TABLE 4

POST-OVERLOAD FATIGUE TEST RESULTS FOR
2091 PLATE AND SHEET

R=0.05 LAB AIR $\Delta K=6.0 \text{ ksi}(\text{in})^{.5}$ ONE OVERLOAD CYCLE APPLIED

<u>% O.L.</u>	<u>a/W</u>	<u>Pcl/Pmax</u>	<u>da/dN @ O.L.</u> <u>(u-ln/cyc)</u>	<u>DELAY CYCLES</u> <u>(x10⁻³)</u>
PLATE (.250 thick)				
80	0.369	0.402	0.184	171.7
80	0.463	0.456	0.199	146.7
80	0.559	0.449	0.414	93.4
80	0.600	0.386	0.399	85.8
PLATE (.140 thick)				
80	0.401	0.645	0.097	arrest
80	0.447	0.603	0.095	arrest
60	0.407	0.535	0.135	137.6
60	0.415	0.640	0.076	arrest
60	0.484	0.584	0.057	891.0
60	0.502	0.647	0.149	126.7
60	0.541	0.600	0.140	72.8
60	0.654	0.523	0.120	59.0
60	0.696	0.574	0.107	71.5
SHEET (.140 thick)				
60	0.264	0.516	1.227	13.2
60	0.276	0.511	0.696	31.6
60	0.314	0.505	2.435	17.4
60	0.315	0.501	1.381	19.7
60	0.349	0.483	1.133	30.3
60	0.368	0.45	2.495	13.8
60	0.400	0.413	2.331	22.0
60	0.447	0.446	1.624	14.3
60	0.516	0.379	3.143	11.6
60	0.574	0.344	3.527	10.3

Al 2091-T851

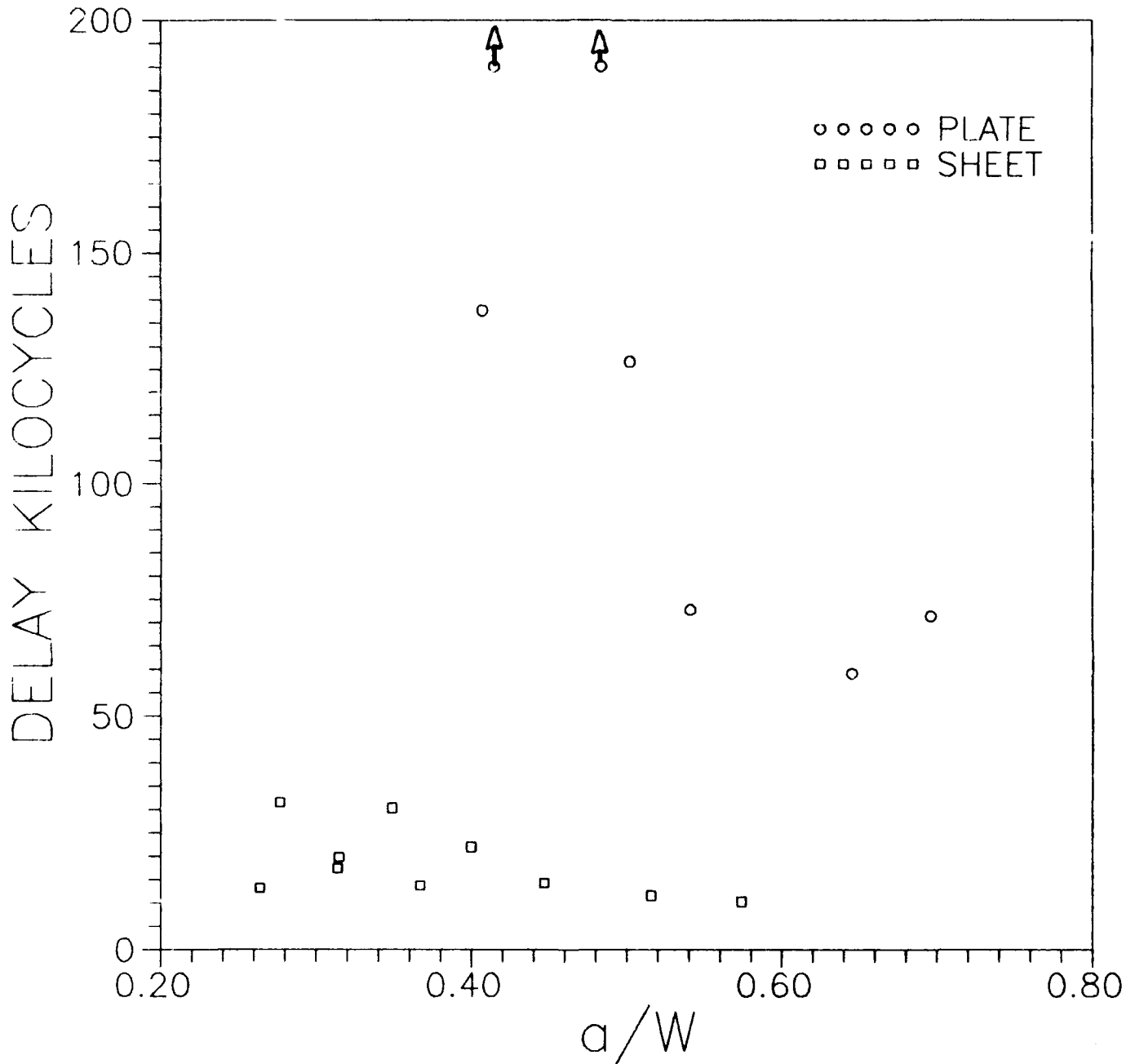


Figure 4. A Comparison of Delay Cycles Due to Fatigue Crack Growth Retardation for a 60 Percent Overload Cycle at a Stress Intensity of $6 \text{ KSI}\sqrt{\text{in}}$ in 2091-T81 Plate Versus 2091-T83 Sheet. Thickness of the Compact Tension Specimens Used for Plate and Sheet was 0.144 Inch.

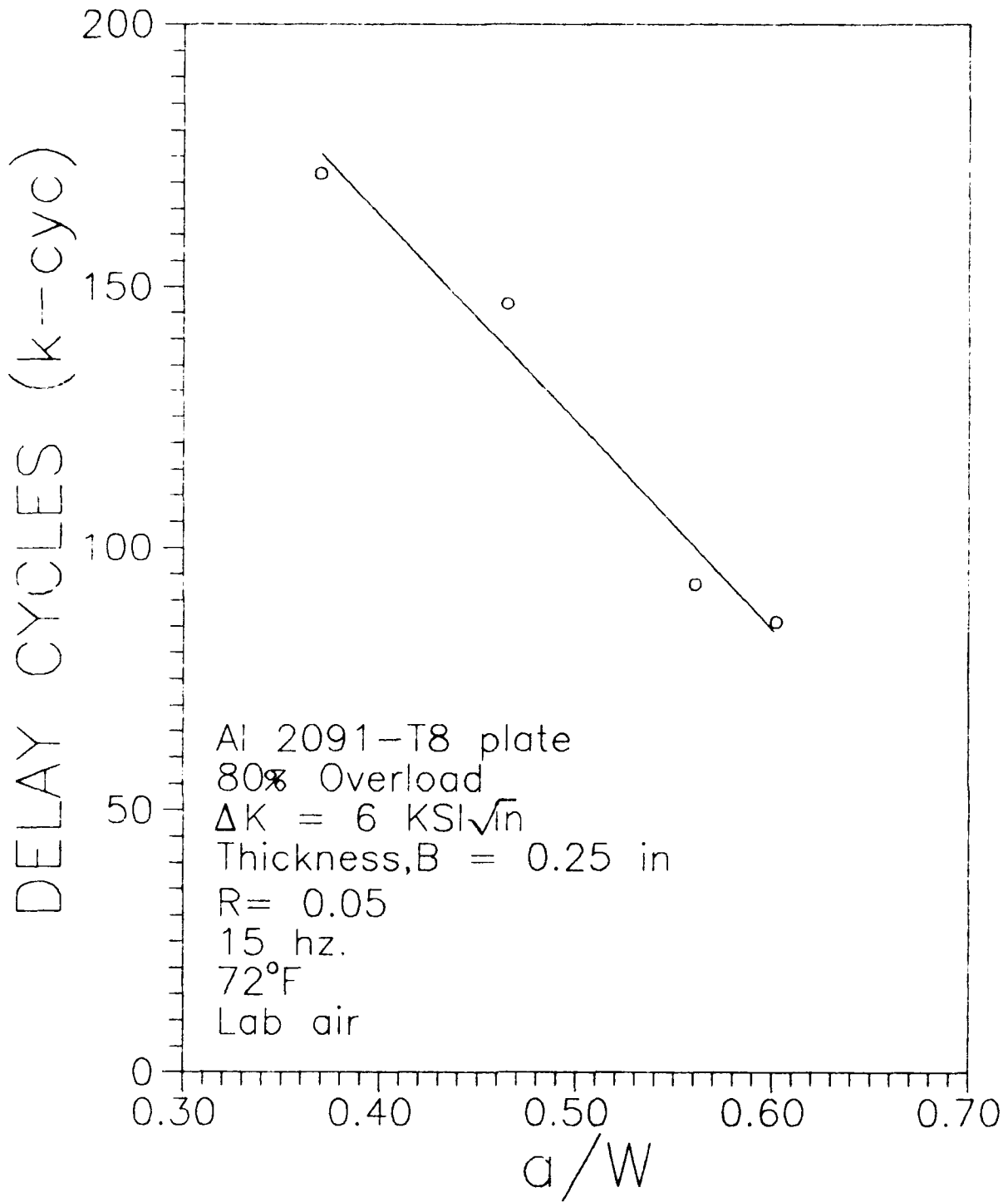


Figure 5. Delay Cycles Due to Fatigue Crack Growth Retardation for an 80 Percent Overload Cycle at a Stress Intensity Range of $6 \text{ KSI}\sqrt{\text{in}}$, in 2091-T81 Plate, with a Specimen Thickness of 0.250 Inch.

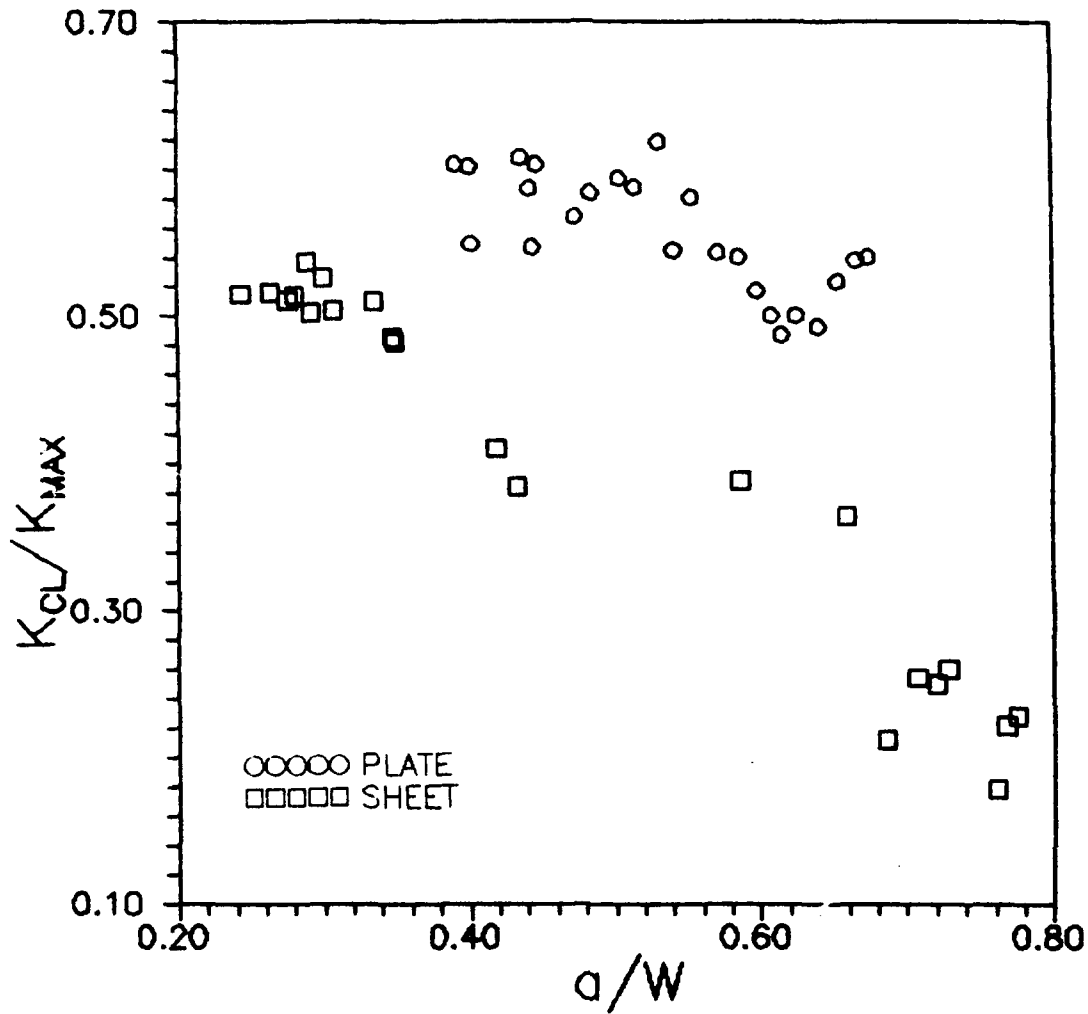
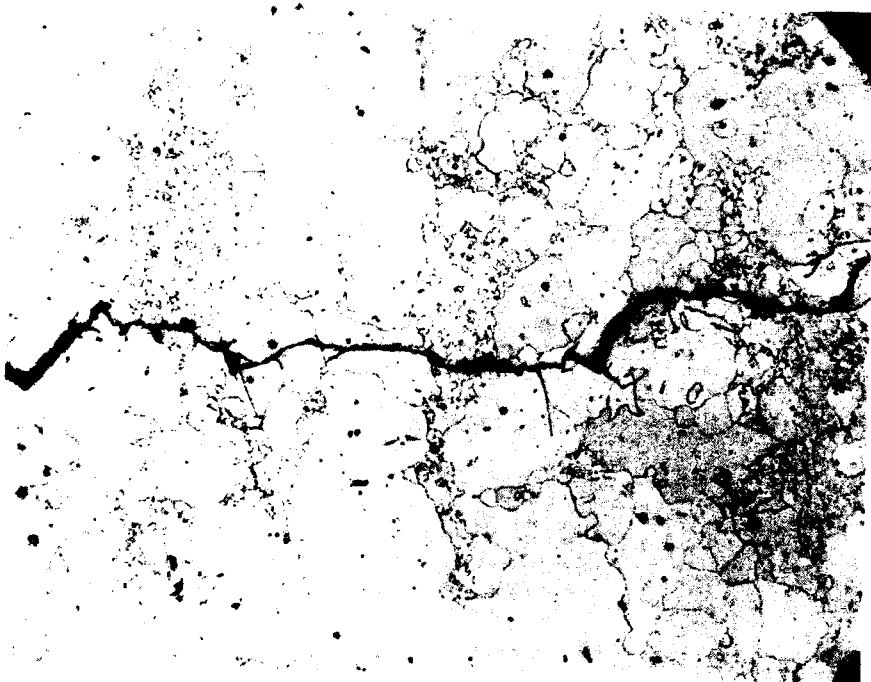


Figure 6. A Comparison of the Crack Closure Level Prior to the Application of a 60 Percent Overload Cycle. Note the Larger Level of Crack Closure in the Plate as Compared to Sheet Which Correlates With the Overload Delay Cycles in Figure 2.



LT8 (100X)



L33 (100X)

Figure 7. (a) Fatigue Crack in Alloy 2091-T81 Plate, and
(b) in Alloy 2091-T83 Sheet at 100X.

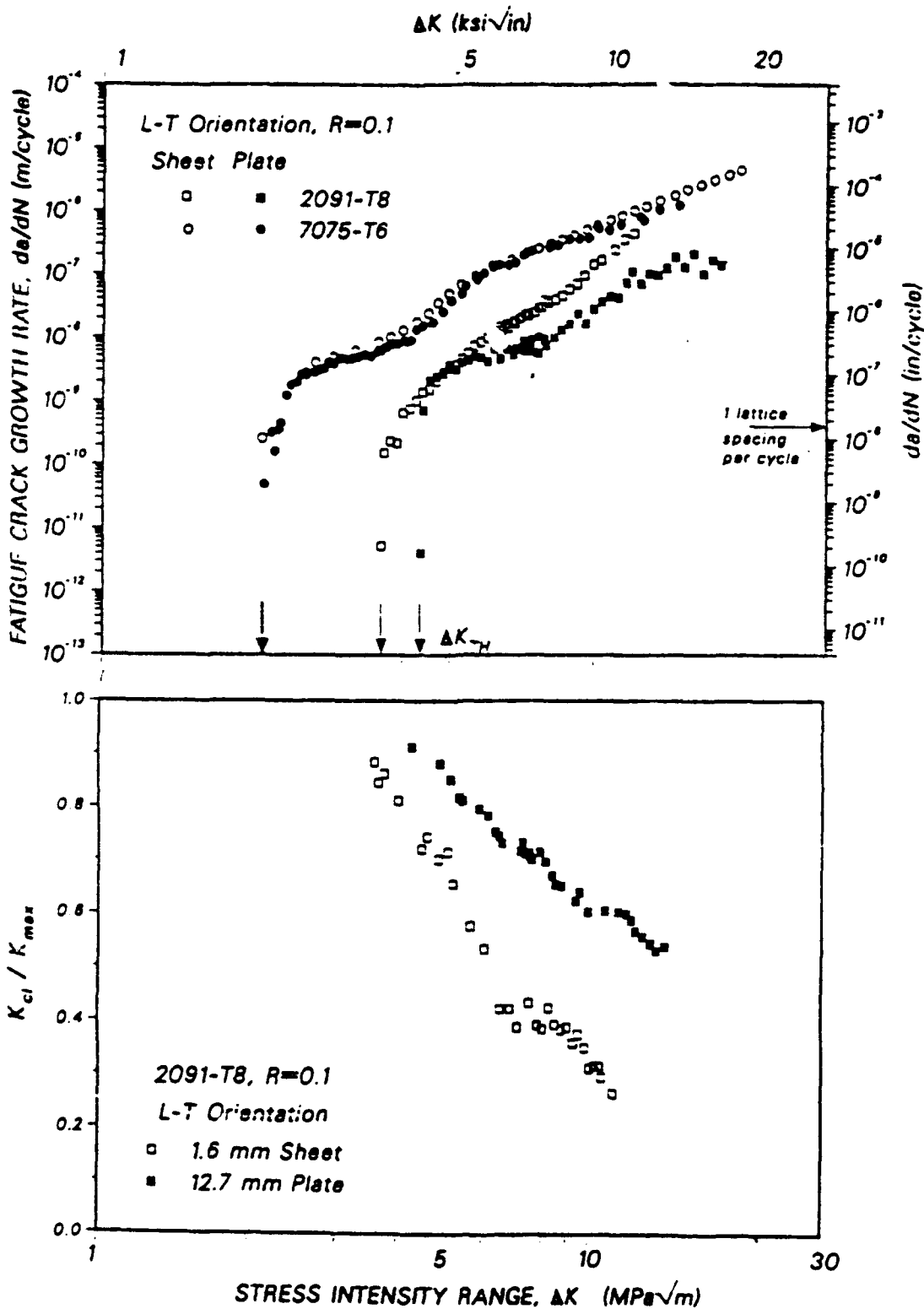


Figure 8. (a) Fatigue Crack Growth Rates and (b) Normalized Crack Closure Levels in 2091-T8 Sheet and Plate, in the L-T Orientation at R=0.1, as a Function of Stress Intensity Range. Reproduced from Reference (1).

Table 5 presents the crack extension required for the post-overload velocity to recover. In general, for the sheet, following the overload the crack immediately accelerated into the plastic zone which was followed by the retardation load cycles, as shown in Figure 9. Whereas in the plate material, following a 60 percent overload, the crack would slow almost immediately, illustrated in Figure 10, and then recover. For a more severe overload, 80 percent, the crack front accelerating into the plastic zone also became evident in the plate material, as presented in Figure 11 and Table 5. Even though the plate required a considerably greater number of load cycles for the velocity to recover, the concomitant post-overload crack extension was equal or slightly less than that required for the sheet to recover.

TABLE 5

POST-OVERLOAD RECOVERY CRACK EXTENSION
IN 2091 PLATE AND SHEET

$\Delta K = 6.0 \text{ ksi}(\text{in})^{.5}$ 15 hz. Lab Air		R = .05	One Overload Cycle Applied Crack Tip Plastic Zone = 0.004 (in)	
<u>a/W</u>	<u>da/dN @ O.L.</u> (u-In/cyc)	<u>Accelerate into</u> <u>Plastic Zone?</u>	<u>Post O.L. Recovery</u> <u>delta-A (in)</u>	
PLATE (.250 in. thick) 80 PERCENT OVERLOAD				
0.369	0.184	Yes	0.020	
0.463	0.199	Yes	0.025	
0.559	0.414	Yes	0.025	
0.600	0.399	Yes	0.015	
PLATE (.144 in. thick) 80 PERCENT OVERLOAD				
0.401	0.097	Yes	arrest	
0.447	0.095	No	arrest	
PLATE (.144 in. thick) 60 PERCENT OVERLOAD				
0.407	0.135	No	0.015	
0.415	0.078	No	arrest	
0.484	0.057	No	0.024	
0.502	0.149	No	0.016	
0.541	0.140	No	0.015	
0.654	0.120	No	0.009	
0.696	0.107	Yes	0.016	
SHEET (.144 in. thick) 60 PERCENT OVERLOAD				
0.246	1.227	Yes	0.016	
0.276	0.696	Yes	0.015	
0.314	2.435	Yes	0.042	
0.315	1.381	Yes	0.020	
0.349	1.133	No	0.020	
0.368	2.495	Yes	0.026	
0.400	3.331	Yes	0.025	
0.447	1.624	Yes	0.016	
0.516	3.143	No	0.020	
0.574	3.527	Yes	0.026	

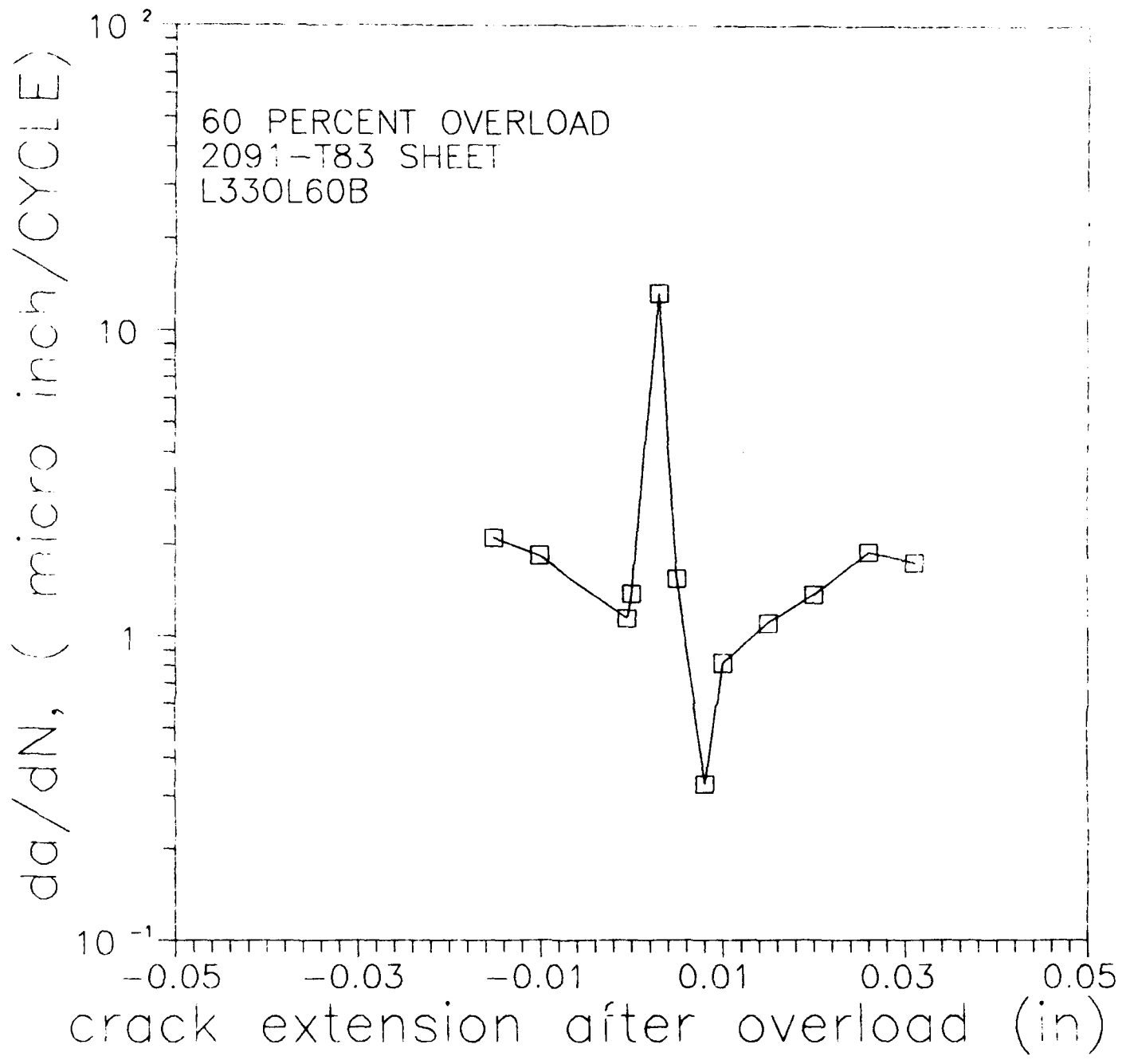


Figure 9. Crack Velocity Versus Post-Overload Crack Extension for Alloy 2091-T83 Sheet.

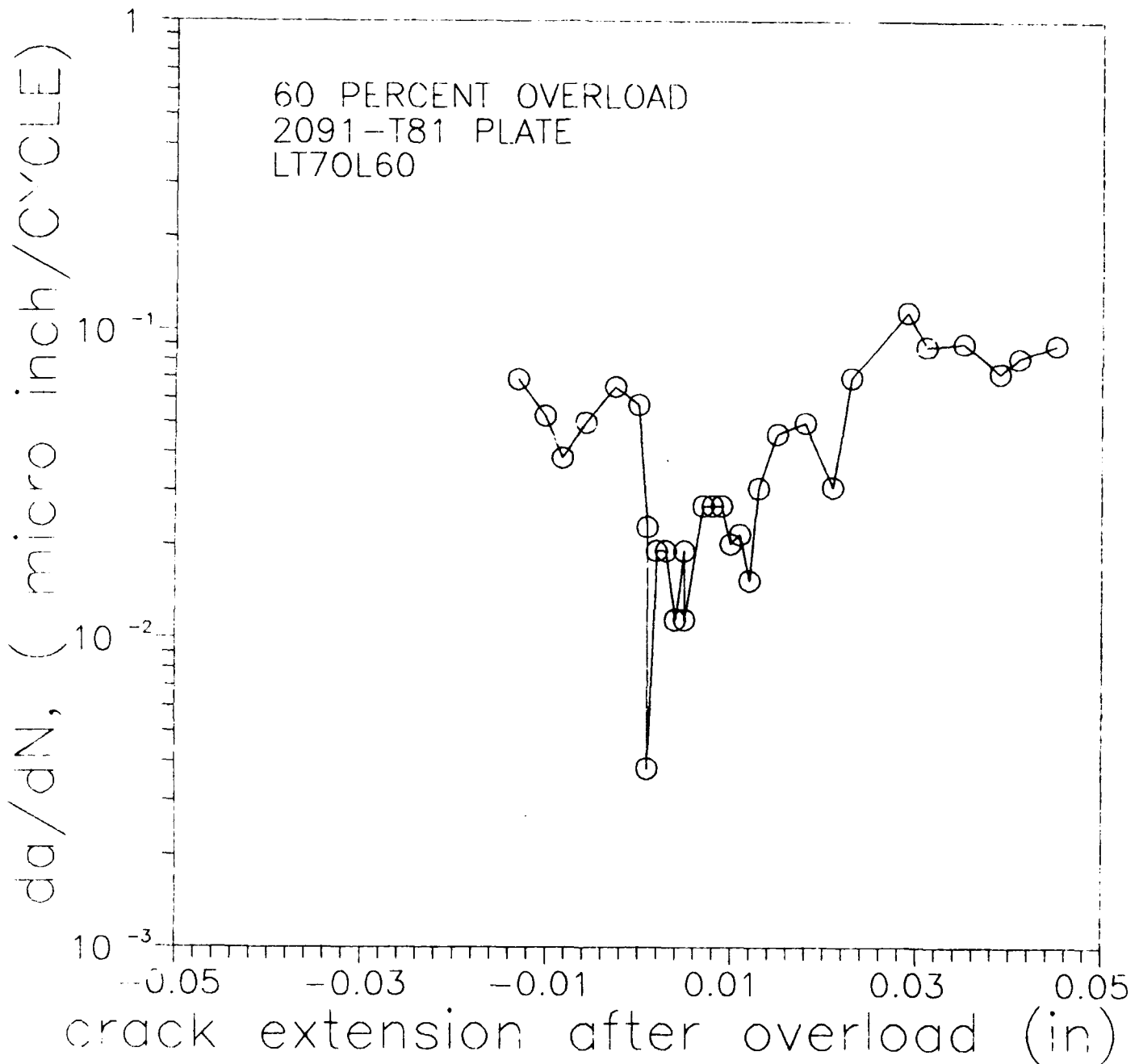


Figure 10. Crack Velocity Versus Post-Overload Crack Extension for Alloy 2091-T81 Plate 0.144 Inch Thick.

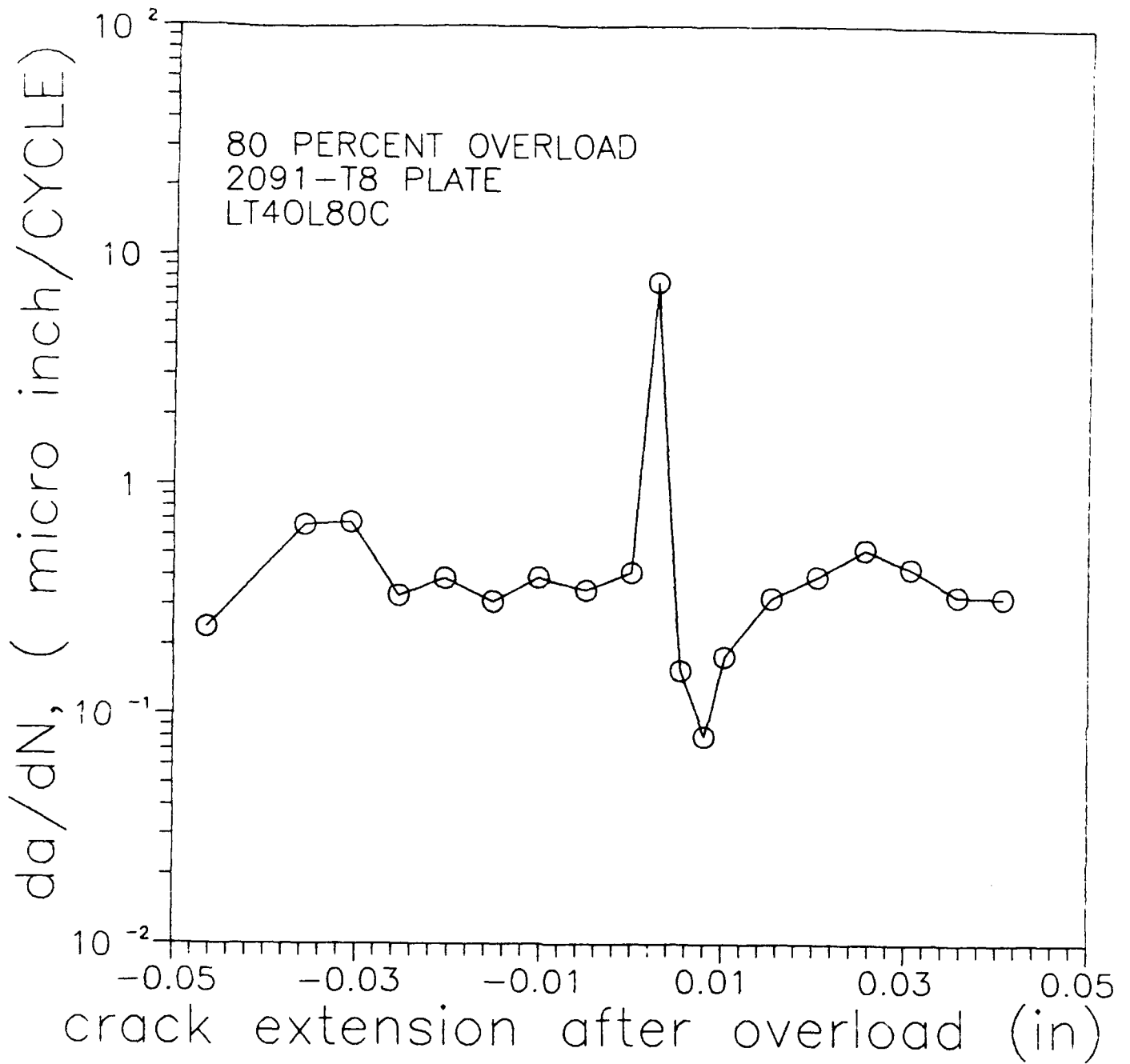


Figure 11. Crack Velocity Versus Post-Overload Crack Extension for Alloy 2091-T81 Plate 0.250 Inch Thick.

SECTION 6 CONCLUDING REMARKS

The effect of a single 60 percent overload fatigue cycle on the fatigue crack growth rate in 2091 plate and sheet in T8 temper has been investigated at 6 KSI $\sqrt{\text{in}}$. Dual location back-face-strain gage technique was employed to measure far-field closure. The following conclusions can be drawn from the present work.

1. The plate material showed substantially higher crack closure levels and higher number of post-overload cycles (i.e., number of delay cycles) to attain the preoverload crack velocity.
2. The number of delay cycles varied significantly with the starting crack length. Larger crack lengths resulted in reduced number of delay cycles. On the other hand, the sheet material did not exhibit the same effect; the variation of number of delay cycles changed only slightly with crack length.
3. A correlation between the far-field crack opening loads and delay cycles could not be found; there was no significant change in the crack closure level after the application of overload and during the recovery period for either material.

SECTION 7
REFERENCES

1. Venkateswara Rao, K.T., Bucci, R.J., Jata, K.V., and Ritchie, R.O., "A Comparison on Fatigue-Crack Propagation Behavior in Sheet and Plate Aluminum-Lithium Alloys," to be published in Materials Science and Engineering, 1991.
2. Jata, K.V. and Ruschau, J., "Effect on Orientation and Aging on Mechanical Properties of Aluminum-Lithium 2091 Sheet," "Light Weight Alloys for Aerospace Applications," Edited by E.W. Lee, et al., pp. 195-207, 1989.
3. Maxwell, D.C., "Strain Based Compliance Method for Determining Crack Length for a C(T) Specimen," AFWAL-TR-87-4096, July 1987.
4. Cervay, R.R., "Post-Overload Fatigue Crack Recovery in Powder Metal Aluminum-Lithium Al 905XL Forging," WR-TR-91-4008, October 1990.
5. Venkateswara Rao, K.T. and Ritchie, R.O., Center for Advanced Materials, "Mechanics for Retardation on Fatigue Cracks Following Single Tensile Overloads: Behavior in Aluminum Lithium Alloys," Submitted to Acta Metallurgical, September 1987.